

DESIGN OF HETEROPOLY COMPOUND-IMBEDDED POLYMER FILM CATALYSTS AND THEIR APPLICATION

Wha Young Lee[†], In Kyu Song*, Jong Koog Lee,
Gyo Ik Park and Seong Soo Lim

Department of Chemical Engineering, Seoul National University, Shinlim-dong, Kwanak-ku, Seoul 151-742, Korea

*Department of Industrial Chemistry, Kangnung National University, Kangnung, Kangwondo 210-702, Korea

(Received 18 September 1997 • accepted 27 November)

Abstract – Heteropolyacid-imbedded polymer film catalysts were applied for the vapor-phase catalytic reaction. Thin film catalysts were prepared by membrane technology using homogeneous heteropolyacid-polymer solutions. It was found that heteropolyacid was finely and uniformly dispersed throughout the polymer matrix. Heteropolyacid catalyst could be designed by this method to enhance acid or oxidation catalysis. Future aspects of the film catalyst were also described in this work.

Key words: Heteropolyacid, Polymer, Catalyst Design, Application

INTRODUCTION

Heteropolyacids (HPAs) are inorganic acids as well as oxidizing agents [Song et al., 1991; Kozhevnikov, 1995; Okuhara et al., 1996]. They are highly soluble in polar solvents such as water, alcohols and amines, but some HPAs are insoluble in non-polar chemicals such as benzene and olefins [Kozhevnikov and Matveev, 1983; Misono et al., 1988; Song et al., 1992]. The solubility of HPAs in turn is closely related to their ability to adsorb reactants. Polar substances readily penetrate into the bulk of HPAs to form a pseudo-liquid phase [Misono et al., 1980; Lee et al., 1992], whereas non-polar chemicals are mostly adsorbed on the surface of HPAs [Misono et al., 1988]. Owing to these characteristics, HPAs have been widely investigated and used in a commercial process producing methacrylic acid [Lee, 1979; Konishi et al., 1982; Kim et al., 1985]. It is well known [Ai, 1982; Kim et al., 1991; Mizuno and Misono, 1994; Song et al., 1994, Hill and Prosser-McCartha, 1995] that the acidic and redox properties of HPA can be controlled in a systematic way by replacing the protons with metal cations and/or by changing the heteroatom or the framework transition-metal atoms.

Novel catalysis of HPA has been also modified by combining HPA with polymer materials [Nomiya et al., 1986]. Some examples for the application of HPA together with polymer materials to the separation processes have been reported. It was reported [Pozniczek et al., 1991] that $H_3PMo_{12}O_{40}$ -doped polyacetylene film catalyst showed a higher oxidation activity and a higher acid-catalytic activity for the ethanol conversion than bulk $H_3PMo_{12}O_{40}$. The enhanced activities for both reactions were explained in terms of dispersion and modification of HPA through the conductive polyacetylene film. Another work [Hasik et al., 1994] was done on the

$H_3PW_{12}O_{40}$ -dispersed polyaniline catalyst which was prepared by polymerizing aniline together with HPA. It was reported that the HPA-polyaniline catalyst showed a higher oxidation activity but a lower acid-catalytic activity for the isopropanol conversion because heteropolyanion was strongly combined with polyaniline. One example for the application of HPA-polymer system to the gas separation process could be found in the literature [Lee et al., 1995]. HPA was blended with polyvinylalcohol using water as a common solvent to prepare the single-phase membrane for H_2 separation.

Another method for the modification of novel catalysis of HPA reported by this group [Song et al., 1993, 1994; Lee et al., 1996, 1997] is to blend HPA with polymer using solvents to form a membrane-like film catalyst. Acidic and redox properties of HPA could be easily controlled by this method to meet the need for the specific reactions. Some examples for the application of HPA-blended polymer film catalysts to the vapor-phase catalytic reaction were demonstrated in this work. HPA-blended polymer film catalysts were prepared by membrane technology, and they were tested as fixed-bed catalysts in a continuous flow reactor. Feasible applications of HPA-polymer system were also described.

EXPERIMENTAL

1. Preparation of HPA-Imbedded Polymer Film

$H_3PMo_{12}O_{40}$ (PMo, Aldrich) was purified and calcined at 300 °C for precise quantification. Polysulfone (PSF, Udel-1700 from Union Carbide), polyethersulfone (PES, Victrex 5200P from ICI), and polyphenylene oxide (PPO, poly-2,6-dimethyl-1,4-phenylene oxide from Aldrich) were used as blending polymers. Dimethylformamide (DMF) or mixture of methanol (M) and chloroform (C) was used as a blending solvent. A homogeneous PMo-polymer-solvent solution was prepared at room temperature. This solution was casted on a glass

[†]To whom all correspondence should be addressed.
E-mail:wyl@plaza.snu.ac.kr

plate with a constant thickness in ambient condition to form a membrane-like film catalyst. All the dried film catalysts were thermally treated before reaction and characterization.

2. Reaction and Characterization

Vapor-phase ethanol (or propanol) conversion was carried out in a continuous flow reactor. The film catalyst was cut into small pieces (2 mm × 2 mm) and used as a fixed-bed catalyst. All the film catalysts were treated at 170 °C for 1 hr by passing air (5 cc/min) before the reaction. Ethanol (or propanol) was preheated for vaporization and fed to the reactor together with a carrier gas. Air was used for the oxidation and helium was used for the acid-catalyzed reaction. The products were analyzed under a steady state condition with an on-line GC (HP 5890 II). Conversions and selectivities were calculated on the basis of carbon balance. The film catalysts were characterized by IR (Midac Co. M2000), TPD, SEM (Jeol JMS-35), EDX (Philips PV-9900), DSC (TA Instruments TA 200), and ESCA (Perkin-Elmer PHI 581). All the film catalysts were thermally stable during the reaction because the reaction was carried out at temperatures below the glass transition temperature (T_g) of corresponding polymers.

CHARACTERISTICS OF FILM CATALYST

1. Characteristics of PMo-PSF-DMF

A homogeneous PMo-PSF-DMF solution was successfully obtained by dissolving both PMo and PSF in a common solvent of DMF. The viscous and greenish PMo (4.76 wt%)-PSF (23.81 wt%)-DMF (71.43 wt%) solution was casted on a glass plate with a constant thickness in ambient condition to form a membrane-like film, and subsequently, it was dried for 4-5 hrs under the same condition. The thickness of the prepared PMo-PSF-DMF film catalyst was 0.017 mm.

The film catalysts comprising PMo and each polymer material show two different thermal behaviors. T_g of a polymer increases when it forms a physicochemical blending with PMo, but, on the other hand, T_g of some polymers decreases when it forms a physical blending [Lee et al., 1996]. Fig. 1 shows the thermal behavior of PMo-PSF-DMF and PSF-DMF (PMo-free film). T_g of PSF-DMF and PMo-PSF-DMF were found

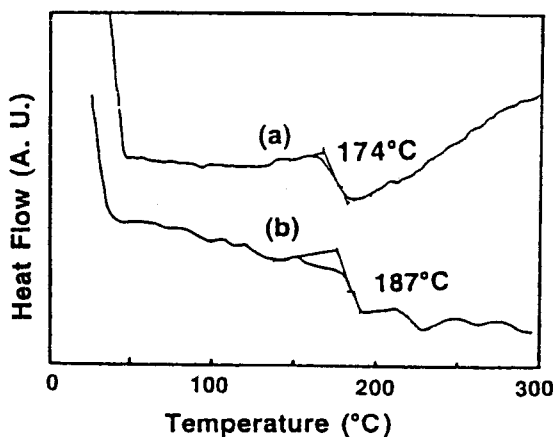


Fig. 1. Thermal behavior of (a) PMo-PSF-DMF and (b) PSF-DMF.

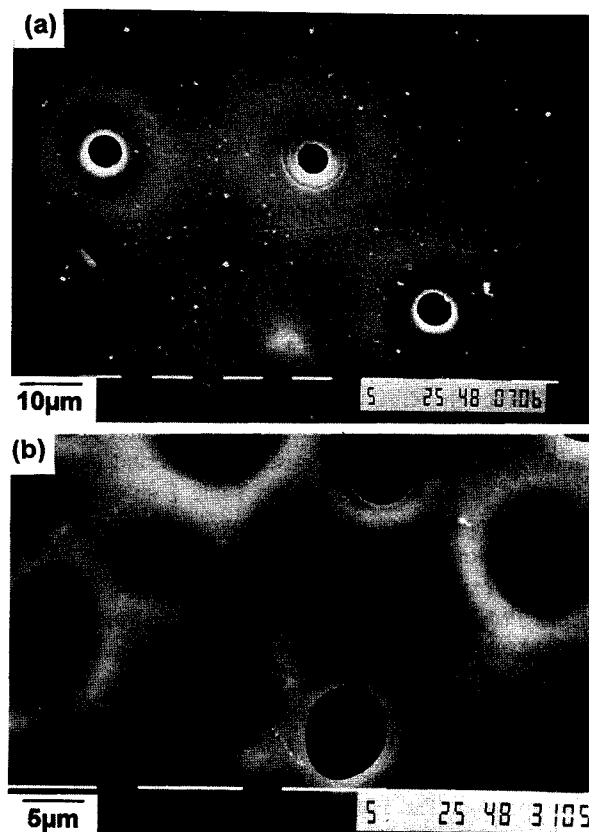


Fig. 2. SEM images of (a) PSF-DMF and (b) PMo-PSF-DMF.

to be 187 °C and 174 °C, respectively. These results mean that PMo in PMo-PSF-DMF acts as an impurity and that the blending of PMo with PSF is physical. The physical blending was also confirmed from IR measurements. Typical bands of the Keggin structure of PMo in the PMo-PSF-DMF film were not changed. Fig. 2 shows the SEM micrographs of PSF-DMF and PMo-PSF-DMF film. No visible evidence representing PMo was found in the PMo-PSF-DMF film and there was no distinctive difference between PSF-DMF and PMo-PSF-DMF. This indicates that PMo was not recrystallized into large particles but was finely dispersed as fine particles invisible in the SEM in the PMo-PSF-DMF. The uniform distribution of PMo in the PMo-PSF-DMF film was also confirmed by EDX analysis, as shown in Fig. 3.

In order to investigate any interaction between PMo and PSF, the oxidation state of molybdenum in bulk PMo and in PMo-PSF-DMF film was measured by ESCA. The spectrum could be fitted with only one doublet corresponding to Mo 3d_{3/2} and Mo 3d_{5/2}. The binding energies of Mo 3d_{3/2} and Mo 3d_{5/2} in both catalysts were 235.3 eV and 232.1 eV, respectively. Only one type of molybdenum (VI) was confirmed in both PMo and PMo-PSF-DMF. A DMF-TPD experiment on bulk PMo revealed that DMF desorption started at 150 °C and reached the maximum at 270 °C and 337 °C. These temperatures are higher than T_g of PMo-PSF-DMF film. This fact suggests that DMF (organic base) is chemically adsorbed on the acid sites of PMo in the PMo-PSF-DMF film and affects the acidic function of the film catalyst. It is summarized

that highly dispersed PMo catalyst supported on PSF was obtained by blending these two materials. Although the oxidation state of molybdenum of PMo in the PMo-PSF-DMF was not affected, the acidic catalytic activity of the film catalyst might be affected by DMF that was adsorbed on the acid sites of PMo.

2. Characteristics of PMo-Polymer-MC

A new method for the preparation of PMo-embedded polymer film catalyst using mixed solvents was successfully developed toward the modification of novel catalysis of HPA. HPA and polymer can be easily blended if both materials are soluble in a common solvent as in the case of PMo-PSF-DMF. Although HPA and polymer are not soluble in the same solvent, if a solvent dissolving HPA and another solvent dissolving polymer are miscible, HPA and polymer can be blended using solvent mixture. Table 1 shows the typical solubility properties of PMo and several polymers in methanol and chloroform. Methanol can be used for PMo and chloroform can be used for polymer in this system. A homogeneous PMo (1.22 wt%)-polymer (6.90 wt%)-methanol (4.41 wt%)-chloroform (87.47 wt%) solution was casted on a glass plate in ambient condition, and subsequently, it was dried for 4-5 hrs. The thickness of the film catalyst was 0.017 mm. PSF, PES and PPO were used as blending polymers. PMo-free polymer films were also prepared at the same condition for comparison. The PMo-blended polymer film catalyst was denoted as follows; for example, PMo-blended PSF film catalyst prepared using methanol (M)-chloroform (C) mixture was denoted as PMo-PSF-MC.

Fig. 4 shows the SEM micrographs of bulk PMo and PMo-

Table 1. Solubility properties of $H_3PMo_{12}O_{40}$ and polymers

	Methanol (M)	Chloroform (C)
$H_3PMo_{12}O_{40}$ (PMo)	Soluble	Insoluble
Polysulfone (PSF)	Insoluble	Soluble
Polyethersulfone (PES)	Insoluble	Soluble
Polyphenylene oxide (PPO)	Insoluble	Soluble

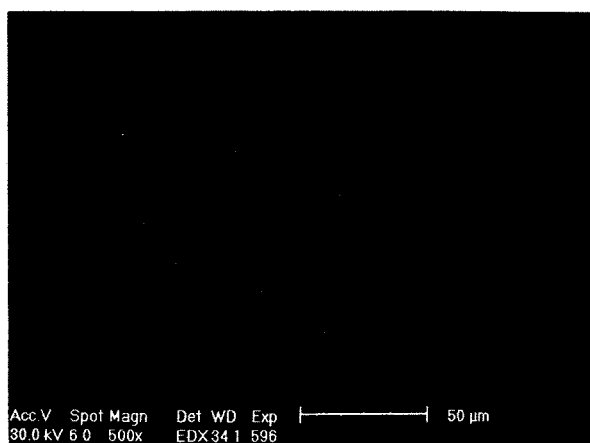


Fig. 3. EDX image of PMo-PSF-DMF film by mapping on only molybdenum.

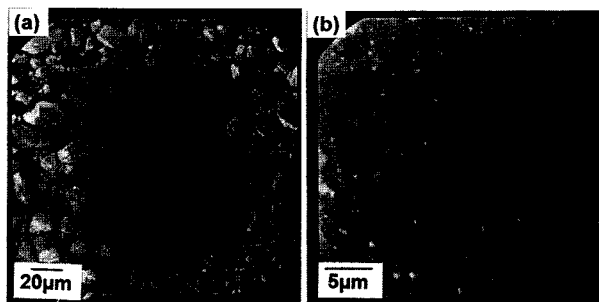


Fig. 4. SEM images of (a) bulk PMo and (b) PMo-PPO-MC.

Table 2. Glass transition temperatures of various polymer films and PMo-polymer films

Film or film catalyst	Glass transition temperature (°C)
PSF-MC	184
PMo-PSF-MC	<180
PES-MC	236
PMo-PES-MC	219
PPO-MC	211
PMo-PPO-MC	221

Heating rate=15 °C/min

PPO-MC film catalysts. The bulk PMo was large clusters with diameters of 10-100 μm . All the film catalysts retained a greenish color implying fine dispersion of PMo throughout each polymer matrix. No visible evidence for PMo in PMo-PSF-MC and in PMo-PES-MC was found in the SEM images as in the case of PMo-PSF-DMF. This will be discussed in detail later. This result indicates that PMo is uniformly and finely dispersed throughout PSF and PES matrices. On the other hand, PMo in PMo-PPO-MC exists as agglomerates having diameters of 1 μm or less, although PMo dispersion is much improved compared to the bulk PMo.

Glass transition temperatures of various films and film catalysts are listed in Table 2. T_g of PES-MC was 236 °C whereas that of PMo-PES-MC was 219 °C. T_g of PMo-PSF-MC was not detected from room temperature to 350 °C. However, considering that the physical state of PMo-PSF-MC was changed after the reaction over 180 °C and became fragile, T_g of PSF was supposed to be lowered after blending with PMo. The decreased T_g of PSF and PES after blending with PMo means that there is no interaction or no chemical bonding between PMo and polymer in the film catalyst, and PMo acts as an impurity for each polymer as in the case of PMo-PSF-DMF. The increased T_g of PPO after blending with PMo suggests that there is a certain interaction between PMo and PPO and that PMo is not an impurity for PPO. Chemical state of PMo-PPO-MC is not clear, but it can be presumed that PMo-PPO-MC may show a different catalytic activity from PMo-PSF-MC and PMo-PES-MC.

ESCA measurement showed that the binding energies of Mo $3d_{3/2}$ and Mo $3d_{5/2}$ in PMo and PMo-PSF-MC were 235.3 eV and 232.1 eV, respectively. It was confirmed that there was only one type of molybdenum (VI) in both PMo and PMo-PSF-MC like PMo-PSF-DMF.

Table 3. Catalytic activity of PMo-PSF-DMF at 170 °C

Catalyst	EtOH conversion (%)	Amount of EtOH converted to product ($\times 10^4$ moles/g-PMo-hr)		
		CH ₃ CHO	C ₂ H ₄	C ₂ H ₅ OC ₂ H ₅
Bulk PMo ^{a)}	2.7	0.69	0.42	3.0
PMo-DMF ^{b)}	1.5	1.50	0.19	0.50
PMo-PSF-DMF ^{c)}	6.2	7.44	0.49	1.39

W/F=66.73 g-PMo-hr/EtOH-mole, air=5 cc/min, film thickness=0.017 mm, ^{a)}bulk PMo was treated at 300 °C before reaction, ^{b)}PMo was recrystallized from dimethylformamide and then treated at 170 °C before reaction, ^{c)}film catalyst was treated at 170 °C before reaction

Table 4. Catalytic activity of PMo-polymer-MC at 170 °C

Catalyst	EtOH conversion (%)	Amount of EtOH converted to product $\times 10^4$ moles/g-PMo-hr (Carbon selectivity)		
		CH ₃ CHO	C ₂ H ₄	C ₂ H ₅ OC ₂ H ₅
Bulk-PMo ^{a)}	6.9	0.52 (12.8)	0.34 (8.4)	3.22 (78.8)
PMo-MC ^{b)}	7.4	0.46 (10.5)	0.38 (8.6)	3.54 (80.9)
PMo-PSF-MC ^{b)}	39.5	4.67 (20.0)	3.76 (16.1)	14.93 (63.9)
PMo-PES-MC ^{b)}	33.7	1.79 (9.0)	6.46 (32.4)	11.68 (58.6)
PMo-PPO-MC ^{b)}	13.4	4.71 (59.4)	0.78 (9.8)	2.44 (30.8)

W/F=169.1 g-PMo-hr/EtOH-mole, air=5 cc/min, film thickness=0.017 mm, ^{a)}bulk PMo was treated at 300 °C before reaction, ^{b)}PMo was recrystallized from methanol-chloroform mixture and then treated at 170 °C before reaction, ^{c)}film catalyst was treated at 170 °C before reaction

OXIDATION CATALYSIS

1. Catalytic Activity of PMo-PSF-DMF

Table 3 shows the catalytic activity of bulk PMo and PMo-PSF-DMF film catalysts at 170 °C. Acetaldehyde is formed by oxidation, while ethylene and diethylether are formed by acid-catalyzed reaction over the PMo catalyst. As shown in Table 3, the PMo-PSF-DMF film catalyst showed a higher ethanol conversion than the bulk PMo. The PMo-PSF-DMF showed a remarkably enhanced yield and selectivity for acetaldehyde, but it showed a decreased activity for acid-catalyzed reaction compared to the bulk PMo. The oxidation activity of the film catalyst was about 10 times higher than that of the bulk PMo. It was believed that the enhanced oxidation activity of the film catalyst was due to the fine dispersion of PMo throughout the PSF matrix whereas the reduction of an acidic activity was due to DMF which was strongly adsorbed on the acid sites of PMo. The DMF effect was also confirmed by the catalytic activity of PMo-DMF as listed in Table 3. The above results imply that the film catalyst can be applied to the low temperature oxidation reactions to obtain high yield and selectivity for oxidation product by enhancing PMo dispersion and by suppressing the acid-catalyzed reaction.

2. Catalytic Activity of PMo-Polymer-MC

Ethanol conversion and product selectivities over the film catalysts are listed in Table 4. All the film catalysts showed a higher ethanol conversion than the bulk PMo. The enhanced conversion over the film catalyst is believed to be due to the enhanced surface area of PMo. The conversion was in the following order; PMo-PSF-MC>PMo-PES-MC>PMo-PPO-MC>PMo. PMo-PPO-MC showed the smallest conversion among the three film catalysts, as expected in SEM images of Fig. 4. This may be partly resulted from partial agglomeration

of PMo through the PPO matrix. Bulk PMo and PMo-MC showed similar conversion and selectivity. This means that the mixed solvent has no influence on the catalytic activity of PMo unlike DMF of the PMo-PSF-DMF. It also suggests that the main reason for the enhanced activity of the film catalyst is not the effect of mixed solvent but the enhanced PMo dispersion upon blending. PMo-PSF-MC and PMo-PES-MC showed enhanced oxidation and acidic catalytic activities compared to the bulk PMo. The selectivity to oxidation over PMo-PPO-MC was three times or more by the other two film catalysts and that to dehydration was 50% or less. Lower surface area of PMo-PPO-MC may be responsible for the lower activity, but different selectivity cannot be explained by the difference in surface area. The increased T_g of PPO after blending with PMo suggests that there is a certain interaction (like chemical bonding) between PMo and PPO. The interaction between two materials can contribute to the inhibition of acidic activity of PMo-PPO-MC.

In order to confirm the individual effect of polymer materials on the catalytic activity, the perm-selectivities of O₂/ethanol through the film catalysts were measured at 80 °C where the extent of reaction was negligible. As shown in Table 5, the ratio of O₂/ethanol in permeation side was smaller than that in the feed side. This means that O₂ permeability

Table 5. Permeability of O₂/ethanol through the film catalyst at 80 °C

Film catalyst	Pressure (atm)	Permeability ratio of O ₂ /ethanol	
		Feed side	Permeation side
PMo-PSF-MC	0.9	1.04	0.57
PMo-PPO-MC	1.1	1.04	0.85
PMo-PES-MC	0.9	1.04	0.11

Permeation area=17.65 cm²

is smaller than ethanol permeability, and the permeation rate of O_2 is the rate-determining step. The lowest ratio of O_2 /ethanol through PMo-PES-MC may be the reason for the lowest acetaldehyde selectivity over PMo-PES-MC. O_2 /ethanol ratio in permeation side and acetaldehyde selectivity showed the same trend in the following order as shown in Table 4 and Table 5; PMo-PPO-MC > PMo-PSF-MC > PMo-PES-MC.

CRYSTAL STRUCTURE AND CATALYST DISPERSION

The secondary structure of solid HPA is a three-dimensional structure where polyanions (primary structure) are connected by water, cations and organic molecules. Owing to the flexible nature of the secondary structure, polar molecules are readily absorbed into the solid bulk by expanding the interstitial space between polyanions. The XRD patterns implying the secondary structure of HPAs differ from one another depending on the amounts of organic molecules coordinated to HPAs [Misono et al., 1988].

Fig. 5 shows the XRD patterns of PMo after various treatments. Bulk PMo was thermally treated at 300 °C under the air flow before XRD measurement. The treated PMo was recrystallized after dissolving it in methanol (M), chloroform (C) and methanol-chloroform (MC) mixture. The ratio of mixed MC in this process was the same as that in film preparation. The extension in Fig. 5 refers to the solvent used. These catalysts were thermally treated at 170 °C under the air stream before XRD measurement. Bulk PMo had a well-defined secondary crystal structure of HPA. PMo-C showed almost the same XRD pattern as bulk PMo. This means that chloroform gives no effect on the secondary structure of PMo. This is because chloroform is a relatively non-polar molecule and is not absorbed in the bulk of PMo. PMo-M had a different secondary structure from the bulk PMo. This is because methanol, a polar molecule, is absorbed in the bulk of PMo even after the thermal treatment at 170 °C. PMo-MC

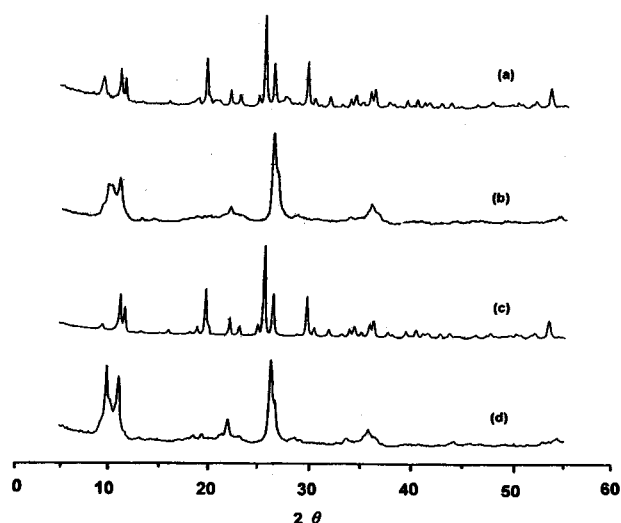


Fig. 5. XRD patterns of (a) bulk PMo, (b) PMo-M, (c) PMo-C and (d) PMo-MC.

also has a modified secondary structure, which is almost the same with that of PMo-M. The above results indicate that chloroform itself gives no effect on the secondary structure of PMo.

Fig. 6 shows the XRD patterns of bulk PMo, PMo-polymer-MC and PMo-PSF-DMF. Bulk PMo and film catalysts were thermally treated at 300 °C and 170 °C, respectively, under the air flow before XRD measurement. PSF, PES and PPO were amorphous polymers, and therefore, they showed no characteristic XRD peaks by themselves. PMo-PSF-MC and PMo-PES-MC showed no XRD peaks as shown in Fig. 6. This indicates PMo was highly dispersed as an amorphous state throughout these film catalysts. However, PMo-PPO-MC showed a modified crystal structure of PMo although XRD peak positions and intensities were quite different from those of bulk PMo. The different XRD patterns of PMo-PPO-MC from those of PMo-PSF-MC and PMo-PES-MC imply the different interactions between PMo and solvents depending on the polymer materials used. This different interaction may affect the formation of different blending patterns of the film catalysts, as described by the thermal analysis in Table 2.

Considering the XRD results in Fig. 6, it is very surprising that PMo-PSF-MC and PMo-PES-MC showed no characteristic XRD peaks. This means that PMo in these film catalysts did not exist as a crystal structure but as an amorphous state. Considering that chloroform is nearly neutral and major part of the mixed solvent is chloroform, it is very difficult to explain why PMo exists as an amorphous state in these film catalysts. It is inferred that this may be due to fine

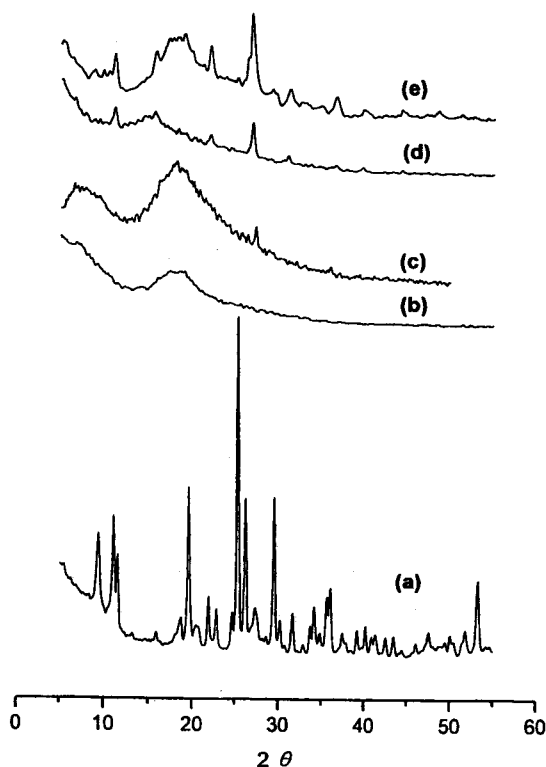


Fig. 6. XRD patterns of (a) bulk PMo, (b) PMo-PSF-MC, (c) PMo-PES-MC, (d) PMo-PPO-MC and (e) PMo-PSF-DMF.

dispersion of PMo catalyst throughout polymer matrix and that there may be some unidentified interactions between PMo and solvents depending on the polymer materials.

It was observed that PMo dispersity throughout polymer matrix also depended on the solvent used. This can be well understood by observing the XRD patterns of PMo-PSF-MC and PMo-PSF-DMF, as shown in Fig. 6. Although the same catalyst and polymer material were used for both film catalysts, PMo-PSF-DMF did not show an amorphous structure but showed a modified crystal structure. It was believed that DMF (polar and basic molecule) was strongly adsorbed on the acid sites of PMo during the blending and remained in the film catalyst even after the thermal treatment at 170 °C. However, PMo in PMo-PSF-DMF did not exist as an amorphous state unlike that in PMo-PSF-MC because of the different PMo dispersity.

ACID CATALYSIS

Steady-state catalytic activities for the ethanol dehydration over PMo-PSF-MC, PMo-PES-MC and PMo-PPO-MC are summarized in Table 6. Helium was used as a carrier gas for this reaction. Ethylene and diethylether were the main products when PMo acted as an acid catalyst.

Bulk PMo and PMo-MC showed a similar ethanol conversion. This means that MC, itself, gives no great effect on the catalytic activity of the bulk PMo. Only a little variation in product yields over PMo-MC from the bulk PMo may be attributed to the modified secondary structure of bulk PMo by the action of MC as evidenced by XRD analysis in Fig. 5. PMo-PSF-MC and PMo-PES-MC showed a higher ethanol conversion compared to the bulk PMo. They also showed remarkably enhanced product yields for the acid-catalyzed reaction. PMo-PES-MC showed the best performance for the acid-catalyzed ethanol dehydration. On the other hand, however, PMo-PPO-MC showed a suppressed ethanol conversion and product yields compared to the bulk PMo.

The enhanced ethanol conversion and product yields over PMo-PSF-MC and PMo-PES-MC are attributed to fine dispersion of PMo throughout the film catalysts. The suppressed ethanol conversion and product yields over PMo-PPO-

MC are attributed to the poor PMo dispersion and the physicochemical interaction of PMo with PPO as shown in Table 2 and Fig. 4.

POROSITY CONTROL

Fig. 7 shows the SEM images of PMo-PSF-DMF and PMo-PSF-MC. PMo-PSF-DMF and PMo-PSF-MC film catalysts were prepared in ambient condition where the relative humidity was 56 %. Water vapor acted as a non-solvent for PSF while DMF or MC was used as a solvent for PSF. There was a distinctive difference in morphology between the two film catalysts. PMo-PSF-MC had no pore-like feature and its surface was very dense and clean whereas PMo-PSF-DMF had well-developed macropores. This result means that phase inversion process occurred differently in two film catalysts [Tsai and Torkelson, 1990; Huang et al., 1995]. Average pore diameter and total surface area of PMo-PSF-DMF were 0.03 μm and 26 m^2/g , respectively.

There are two phases in PSF-solvent system; the PSF-rich phase and the PSF-lean (solvent-rich) phase. Because water is highly miscible with DMF and is non-solvent for PSF, water from ambient condition causes phase separation of PSF-rich phase from DMF-rich phase. This process leads to macropores in PMo-PSF-DMF film catalyst. In the case of PMo-PSF-MC, on the other hand, chloroform is a major component of the mixed solvent and is immiscible with water although water is non-solvent for PSF. Water is not efficient to form macro-

Table 6. Catalytic activity of PMo-polymer-MC at 170 °C

Catalyst	EtOH conversion (%)	Amount of EtOH converted to product $\times 10^4$ moles/g-PMo-hr	
		C_2H_4	$\text{C}_2\text{H}_5\text{OC}_2\text{H}_5$
		Bulk PMo ^a	1.8
PMo-MC ^b	2.3	2.08	5.86
PMo-PSF-MC ^c	23.0	12.3	68.0
PMo-PES-MC ^c	45.9	57.6	100.0
PMo-PPO-MC ^c	1.0	0.93	2.49

W/F=28.69 g-PMo-hr/EtOH-mole, helium=5 cc/min, film thickness=0.017 mm, ^abulk PMo was treated at 300 °C before reaction, ^bPMo was recrystallized from methanol-chloroform mixture and then treated at 170 °C before reaction, ^cfilm catalyst was treated at 170 °C before reaction

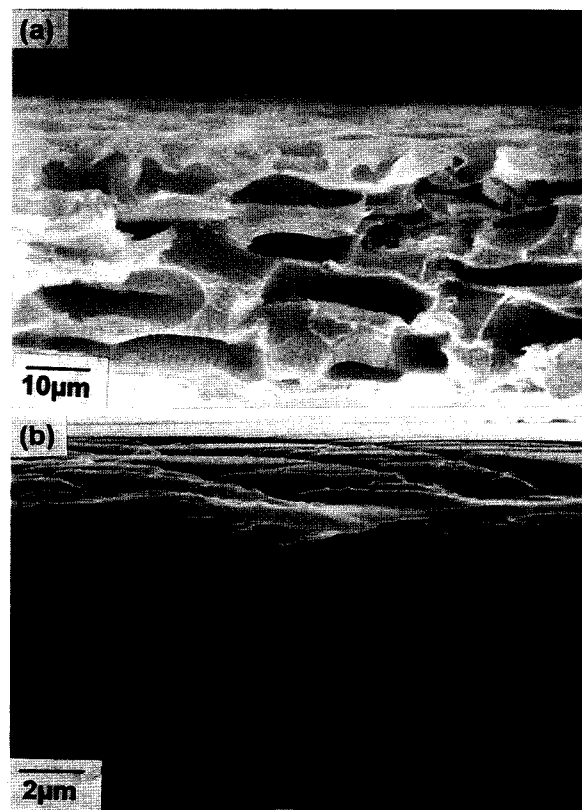


Fig. 7. Cross-sectional SEM images of (a) PMo-PSF-DMF and (b) PMo-PSF-MC.

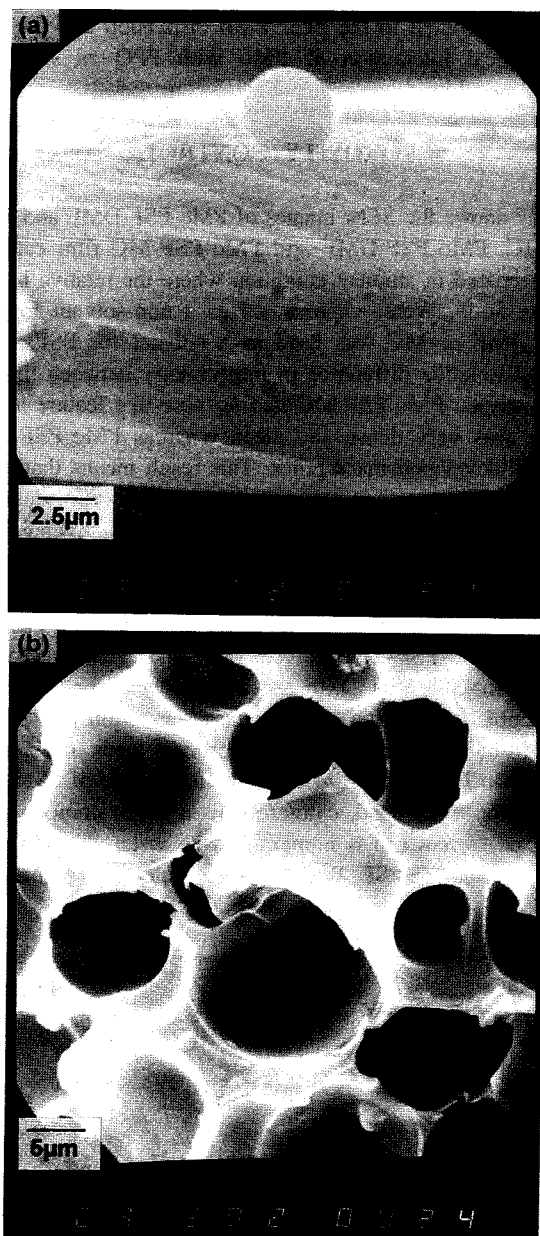


Fig. 8. SEM images of PMo-PSF-DMF: (a) prepared at 56 % relative humidity and dried in vacuum, and (b) prepared and dried at 85 % relative humidity.

pores in PMo-PSF-MC film catalyst.

It was observed that PMo-PSF-DMF which was prepared in ambient condition and dried under vacuum had no pore characteristics as shown in Fig. 8. This was due to rapid removal of DMF and absence of water molecule. The effect of vacuum drying on the pore formation was also confirmed by observing PMo-free PSF-DMF membrane. The PSF-DMF membrane casted in ambient condition turned into a white porous film when it was dried in ambient condition, whereas it turned into a transparent non-porous film after drying under vacuum. PMo-PSF-DMF which was prepared and dried at 85 % relative humidity had well-developed macropores through phase inversion process as shown in Fig. 8. Pore formation and pore characteristics of the film catalyst

are important factors for the reduction of mass transfer resistance in chemical reactions.

APPLICATIONS

A pseudo-catalytic membrane reactor was designed by using PMo (4.76 wt%)-PSF (23.81 wt%)-DMF (71.43 wt%) membrane in order to characterize the film catalyst as a catalytic membrane as shown in Fig. 9. The effective permeation area was 17.65 cm². In this pseudo-catalytic membrane reactor (PCMR) system, no supporting membrane having a separation property was equipped. Vapor-phase 2-propanol conversion was carried out under the air carrier flow. The membrane thickness was 0.24 mm. Propylene is formed by the acidic function of PMo while acetone is produced by the redox catalysis of PMo.

Table 7 shows the catalytic activity of PMo-PSF-PCMR and the ratio of acetone/propylene along with reaction temperature. The formation rate of propylene over PMo-PSF-PCMR was slightly lower than that over PMo. This is attributed to DMF adsorbed on PMo in PMo-PSF-PCMR. PMo-PSF-PCMR showed about 10 times higher acetone yield than PMo because of the enhanced PMo dispersion throughout PSF matrix. It is noteworthy that the ratio of acetone/propylene over PMo-PSF-PCMR was ca. 15 times higher than that over the bulk PMo. The product selectivity was affected by the basic nature of DMF, by the PMo dispersion, and by the permeabilities of product through PMo-PSF-PCMR. It is believed that the higher permeability of acetone (4.05×10^{-8} cm³-cm/cm²-sec-cm Hg at 140 °C) through PMo-PSF-PCMR than propylene (1.94×10^{-8} cm³-cm/cm²-sec-cm Hg at 140 °C) considerably contributed to the increase of acetone yield.

The above-mentioned results imply that HPA-imbedded polymer film catalysts can be used in liquid-phase reactions to meet the need for environmentally benign processes because HPA can be easily recovered after reactions. The HPA-blended

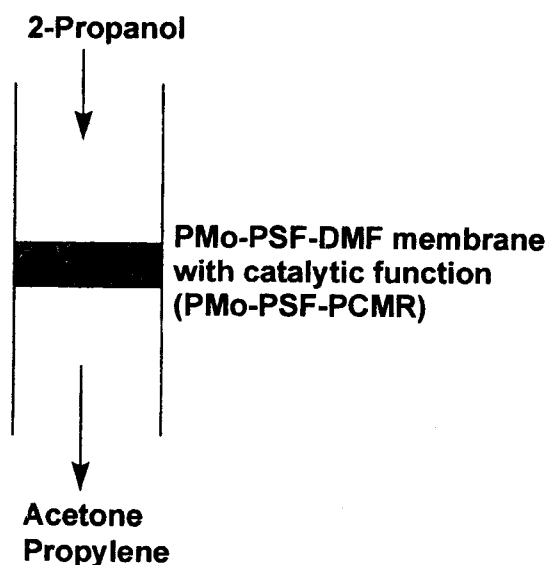


Fig. 9. A schematic diagram of pseudo-catalytic membrane reactor (PCMR) using PMo-PSF-DMF membrane.

Table 7. Formation rate of acetone and propylene over bulk PMo and PMo-PSF-PCMR

Temp. (°C)	Bulk PMo			PMo-PSF-PCMR		
	Acetone ^{a)} × 10 mole/KU ^{a)}	Propylene ^{b)} × 10 mol/KU	Ratio (a/b) × 10 ²	Acetone ^{c)} × 10 mole/KU	Propylene ^{d)} × 10 mol/KU	Ratio (c/d) × 10 ²
120	0.24	26.3	0.91	2.28	17.77	12.83
130	0.43	46.3	0.93	4.58	36.82	12.44
140	0.63	74.7	0.84	6.78	55.21	12.28
150	0.79	95.4	0.83	8.14	78.12	10.42

W/F=21.68 g-PMo-hr/2-propanol-mole, air=3.73 cc/min, membrane thickness=0.24 mm, permeation area=17.65 cm², ^{a)}Keggin Unit

polymer solutions can be also applied to the catalytic membrane reactors as catalytic membranes. Thin composite catalytic membranes can be prepared by casting or coating HPA-blended polymer solution on the supporting polymer membrane. We can take advantage of both modified catalysis of HPA-blended polymer film catalyst and selective separation property of polymer membrane simultaneously. The HPA-blended polymer systems can be also used as catalytic membranes by coating these solutions on the inorganic porous membrane.

CONCLUSIONS

Examples for the application of PMo-blended polymer film catalysts for the vapor-phase catalytic reactions were demonstrated in this work. It was found that PMo was finely and uniformly dispersed throughout the polymer matrix. Conversion and selectivity over the film catalyst were also affected by the nature of solvent and polymer. The film catalyst could be regarded as a highly dispersed HPA catalyst supported on polymer. It was concluded that the film catalyst could be applied to the low temperature oxidations to obtain high yield and selectivity for oxidation products by enhancing catalyst dispersion and by suppressing acid-catalyzed reaction. It was also revealed that acid catalysis of HPA was enhanced by the mutual action of solvent and polymer used. Choosing suitable solvent and polymer was the key step for the modification of novel acid catalysis of HPA in this method. It is expected that HPA-blended polymer film catalysts can be applied to the liquid-phase heterogeneous reaction to meet the need for environmentally benign process. They can be also applied to the membrane reactors as catalytic membranes.

ACKNOWLEDGEMENT

This work has been supported by Daelim Industry Co.

REFERENCES

- Ai, M., "Effects of Cations Introduced into 12-Molybdophosphoric Acid on the Catalyst Properties", *Appl. Catal.*, **4**, 245 (1982).
- Hasik, M., Turex, W., Stochmal, E., Lapkowski, M. and Pron, A., "Conjugated Polymer-Supported Catalysts-Polyaniline Protonated with 12-Tungstophosphoric Acid", *J. Catal.*, **147**, 544 (1994).
- Hill, C. L. and Prosser-McCartha, C. M., "Homogeneous Catalysis by Transition Metal Oxygen Anion Clusters", *Coord. Chem. Rev.*, **143**, 407 (1995).
- Huang, C., Delacruz, M. O. and Swift, B. W., "Phase-Separation of Ternary Mixtures-Symmetrical Polymer Blends", *Macromolecules*, **28**, 7996 (1995).
- Kim, H. C., Moon, S. H. and Lee, W. Y., "Nature and Effect of Counter Cations on the Redox Property of 12-Molybdophosphate", *Chem. Lett.*, 447 (1991).
- Kim, J. J., Rhee, H.-K. and Lee, W. Y., "Oxidation of Methacrolein and Isomerization of *n*-Butene over Heteropoly Compounds", *Chem. Eng. Comm.*, **34**, 49 (1985).
- Konishi, Y., Sakata, K., Misono, M. and Yoneda, Y., "Catalysis by Heteropoly Compounds. IV. Oxidation of Methacrolein to Methacrylic Acid over 12-Molybdophosphoric Acid", *J. Catal.*, **77**, 169 (1982).
- Kozhevnikov, I. V., "Heteropoly Acids and Related Compounds as Catalysts for Fine Chemical Synthesis", *Catal. Rev. -Sci. Eng.*, **37**, 311 (1995).
- Kozhevnikov, I. V. and Matveev, K. I., "Homogeneous Catalysts Based on Heteropoly Acids", *Appl. Catal.*, **5**, 135 (1983).
- Lee, J. K., Song, I. K. and Lee, W. Y., "Separation of H₂/CO by the Selective Sorption Property of H₃PMo₁₂O₄₀ Embedded in PVA Membrane", *Korean J. Chem. Eng.*, **12**, 384 (1995).
- Lee, J. K., Song, I. K., Lee, W. Y. and Kim, J. J., "Modification of 12-Molybdophosphoric Acid Catalyst by Blending with Polysulfone and Its Catalytic Activity for 2-Propanol Conversion Reaction", *J. Mol. Catal.*, **104**, 311 (1996).
- Lee, J. K., Song, I. K., Park, G. I. and Lee, W. Y., "Effect of Solvent on the Catalytic Activity of Heteropoly Acid-Blended Polymer Film Catalyst", *HWAHAK KONGHAK*, **35**, 237 (1997).
- Lee, K. Y., Arai, T., Nakata, S., Asaoka, S., Okuhara, T. and Misono, M., "Catalysis of Heteropoly Compounds. 20. An NMR Study of Ethanol Dehydration in the Pseudoliquid Phase of 12-Tungstophosphoric Acid", *J. Am. Chem. Soc.*, **114**, 2836 (1992).
- Lee, W. Y., "Heteropoly Compounds and Oxidation Catalysts for Methacrolein", *HWAHAK KONGHAK*, **17**, 317 (1979).
- Misono, M., Okuhara, T. and Mizuno, N., "Catalysis by Heteropoly Compounds", *Successful Design of Catalysts*, Inui, T., eds, Elsevier, Amsterdam, 267 (1988).
- Misono, M., Sakata, K., Yoneda, Y. and Lee, W. Y., "Acid-Base Bifunctional Properties of Heteropoly Compounds of Molybdenum and Tungsten Correlated with Activity for

- Oxidation of Methacrolein", New Horizons in Catalysis, Seiyama, T. and Tanabe, K., eds, Kodansha-Elsevier, Amsterdam, 1047 (1980).
- Mizuno, N. and Misono, M., "Heteropolyanions in Catalysis", *J. Mol. Catal.*, **86**, 319 (1994).
- Nomiya, K., Murasaki, H. and Miwa, M., "Catalysis by Heteropolyacids-VIII. Immobilization of Keggin-Type Heteropolyacids on Poly(4-vinylpyridine)", *Polyhedrons*, **5**, 1031 (1986).
- Okuhara, T., Mizuno, N. and Misono, M., "Catalytic Chemistry of Heteropoly Compounds", *Adv. Catal.*, **41**, 113 (1996).
- Pozniczek, J., Kulszewicz-Bajer, I., Zagorska, M., Kruczala, K., Dyrek, K., Bielanski, A. and Pron, A., "H₃PMo₁₂O₄₀-Doped Polyacetylene as a Catalyst for Ethyl Alcohol Conversion", *J. Catal.*, **132**, 311 (1991).
- Song, I. K., Lee, J. K. and Lee, W. Y., "Control of Catalytic Properties of Heteropoly Acid by Blending it with Polymers", *J. Korean Ind. Eng. Chem.*, **5**, 819 (1994).
- Song, I. K., Lee, J. K. and Lee, W. Y., "Preparation and Catalytic Activity of H₃PMo₁₂O₄₀-Blended Polymer Film for the Ethanol Conversion Reaction", *Appl. Catal.*, **119**, 107 (1994).
- Song, I. K., Lee, J. K., Song, J. C. and Lee, W. Y., "Formation and Role of Acid Sites of Heteropoly Acid Catalysts", *J. Korean Ind. Eng. Chem.*, **5**, 431 (1994).
- Song, I. K., Lee, W. Y. and Kim, J. J., "Catalytic Polymer Membranes Prepared by Blending 12-Tungstophosphoric Acid Catalyst and Organic Polymer", *Polymer (Korea)*, **16**, 209 (1992).
- Song, I. K., Moon, S. H. and Lee, W. Y., "Catalytic Activity of Thermally Decomposed 12-Molybdophosphoric and 10-Molybdo-2-vanadophosphoric Acids", *Korean J. Chem. Eng.*, **8**, 33 (1991).
- Song, I. K., Shin, S. K. and Lee, W. Y., "Catalytic Activity of H₃PMo₁₂O₄₀-Blended Polysulfone Film in the Oxidation of Ethanol to Acetaldehyde", *J. Catal.*, **144**, 348 (1993).
- Tsai, F. J. and Torkelson, J. M., "Roles of Phase-Separation Mechanism and Coarsening in the Formation of Poly(Methyl Methacrylate) Asymmetric Membranes", *Macromolecules*, **23**, 775 (1990).